

Contents

Foreword by Edward N. Lorenz vii

Preface xi

Chapter 1

Progress and Problems in Large-Scale Atmospheric Dynamics 1
Isaac M. Held

Chapter 2

Theories of Baroclinic Adjustment and Eddy Equilibration 22
Pablo Zurita-Gotor and Richard S. Lindzen

Chapter 3

The Thermal Stratification of the Extratropical Troposphere 47
Tapio Schneider

Chapter 4

Storm Track Dynamics 78
Kyle L. Swanson

Chapter 5

Eddy-Mediated Interactions Between Low Latitudes and
the Extratropics 104
Walter A. Robinson

Chapter 6

On the Relative Humidity of the Atmosphere 143
Raymond T. Pierrehumbert, H el ene Brogniez,
and R emy Roca

Chapter 7

Quasi-Equilibrium Dynamics of the Tropical Atmosphere 186
Kerry Emanuel

Chapter 8

Simple Models of Ensemble-Averaged Tropical Precipitation and Surface Wind, Given
the Sea Surface Temperature 219
Adam H. Sobel

Chapter 9

Dynamical Constraints on Monsoon Circulations 252
R. Alan Plumb

Chapter 10

Moist Dynamics of Tropical Convection Zones in Monsoons, Teleconnections, and
Global Warming 267
J. David Neelin

Chapter 11

Challenges in Numerical Modeling of Tropical Circulations 302
Christopher S. Bretherton

Chapter 12

Challenges to Our Understanding of the General Circulation:
Abrupt Climate Change 331
Richard Seager and David S. Battisti

List of Contributors 373

Index 375

Chapter 1

Progress and Problems in Large-Scale Atmospheric Dynamics

Isaac M. Held

1.1. Introduction

A theory for the general circulation of the atmosphere has at its core a theory for the quasi-horizontal eddy fluxes of energy, angular momentum, and water vapor by the *macro-turbulence* of the troposphere, as well as a theory for the much smaller-scale convective motions that transport heat and water vertically, especially in the Tropics. A few of the many issues related to convective vertical fluxes are discussed in chapters 7, 8, 10, and 11 in this volume. The focus in this chapter, and of chapters 2–6, 9, and 12, is primarily on the large-scale quasi-horizontal component of the problem. In the Tropics, fluxes by large- and small-scale eddies are so tightly coupled that one cannot easily discuss one without simultaneously discussing the other. But outside of the Tropics, one can hope that a focus on large-scale dynamics in isolation is a meaningful starting point, and it is on the extratropical circulation that I concentrate here.

All of us would love to find a simple variational principle or “fundamental theorem of climate” that solves this problem in a single stroke, but I suspect that most of us are skeptical that such a principle exists. We assume, instead, that the best way of developing theories for a system of this complexity is to construct a hierarchy of models, of varying levels of comprehensiveness, chosen so as to capture the essential sources of complexity with minimal extraneous detail. When confronted with a theory claiming great generality, we expect to see a demonstration that it explains the behavior seen on a number of different levels of our model hierarchy.

An analogy with the use of “model organisms” in biology is informative. Nature has provided us with just the kind of hierarchy, from bacteria to fruit fly to mouse, needed to build up an understanding of our own complex biology. We have no such ready-made hierarchy in climate research, and must instead design and build our own. See Held (2005) for an extended discussion of this analogy and the consequences of the fact that our climate hierarchy is a theoretical construct while the biological hierarchy is provided by nature.

What hierarchy of models should we study so as to best understand how global climate is controlled by external parameters and boundary conditions? The choice of models is centrally important. Only if, as a community, we have selected appropriate models to study collectively will our understanding accumulate efficiently. I personally do not feel that appropriate models can be selected in a systematic way; our physical intuition must guide us towards the most informative models.

In this chapter I will refer to the classic two-layer quasigeostrophic (QG) model, moist QG models, and particular idealized dry and moist primitive-equation models on the sphere. The discussion revolves around the related problems of the poleward eddy heat flux, the effect of latent heat release on midlatitude eddies, and distinctions between the dynamics of the upper and lower troposphere. Considerable space is devoted to the simplest of these models, the two-layer QG model, in an especially simple horizontally homogeneous configuration.

I find this model of homogeneous QG turbulence useful from several perspectives, but there is no claim that the theory for the eddy fluxes in this model is of direct quantitative relevance to the atmosphere. When we talk about the need for a model hierarchy, we are implicitly assuming that the more idealized members of this hierarchy are missing some important ingredients, but that, in spite of these limitations, an understanding of these simpler models is a useful stepping stone to an understanding of their more complex relatives.

1.2. The Two-Layer QG Model

The two-layer QG system provides us with what may be our simplest turbulent “climate” model. The state of this model is determined by the streamfunctions for the non-divergent component of the horizontal flow in two layers of fluid, meant to represent the flow in the upper (ψ_1) and lower (ψ_2) troposphere, the (eastward, northward) components of the velocity being $(u, v) = (-\partial\psi/\partial y, \partial\psi/\partial x)$. In the meteorological context we can think of two isentropic layers of ideal gas with different entropies, or potential temperatures θ , with $\theta_1 > \theta_2$ so as to represent a gravitationally stable system. Hydrostatic and geostrophic balance combine to create Margules’ relation between the perturbations to the height of the interface between the two layers, η , and the difference between the two streamfunctions. In a Boussinesq fluid (with all potential temperatures assumed to be small perturbations away from a constant θ_0) this relation is $f(\psi_1 - \psi_2) = -g^*\eta$, where $g^* \equiv g(\theta_1 - \theta_2)/\theta_0$ is the reduced gravity and f the Coriolis parameter. The dynamics reduces to the advection by these non-divergent flows of a scalar, the QG potential vorticity q_k , within each layer, where

$$q_k = \nabla^2\psi_k + (-1)^k\lambda^{-2}(\psi_1 - \psi_2) + \beta y; \quad k = 1, 2 \quad [1.1]$$

and λ is the radius of deformation, defined by $\lambda^2 = g^*H/f^2$, with H the resting depth of the two layers (assumed to be equal here). The final term in (1.1), with β a constant, is an approximation to the all-important vorticity gradient due to the increase in the radial component of the vorticity of solid body rotation with increasing latitude γ . When relating this two-layer picture to a continuously stratified atmosphere, we think of $(g^*H)^{1/2} \rightarrow NH$, with $N^2 = (g/\theta)\partial\theta/\partial z$ and $-\eta$ as proportional to the vertically averaged potential temperature.

A simple way of creating a statistically steady state is to force the system with mass exchange between the two layers, this model's version of radiative heating, arranged so as to relax the interface to a "radiative equilibrium" shape with a zonally symmetric meridional slope. This mass exchange can be expressed in terms of potential vorticity sources in the two layers. One also invariably includes two types of dissipation: small-scale diffusion is needed to mop up the vorticity variance that cascades to small-scales; and surface friction, damping the low-level vorticity, is needed to remove energy in a non-scale selective manner. Energy does not cascade to small scales in this model and cannot be removed realistically with horizontal diffusion.

Radiative equilibrium is a solution of these equations, with no flow in the lower layer and zonal flow in the upper layer, with the Coriolis force acting on the vertical shear $U = u_1 - u_2$ between the two layers balancing the pressure gradients created by the radiative equilibrium interface slope. This flow is unstable in the absence of the dissipative terms, when the isentropic slope is large enough to overcome β and reverse the sign of the north-south potential vorticity gradient in one of the layers. In flows with temperature decreasing (interface slope rising) with increasing γ , this reversal occurs in the lower layer. If the relative vorticity gradient of the zonal flow is negligible as compared to β , the criterion is the classic one discussed by Phillips more than half a century ago: $\xi \equiv U/(\beta\lambda^2) > 1$. (The supercriticality ξ is the two-layer counterpart to the parameter S_c used in chapter 3.) The existence of this critical slope presents us with a problem, since analogous models of inviscid baroclinic instability in continuously stratified atmospheres are unstable for any nonzero vertical shear (or isentropic slope). (In multilayer models, the critical interfacial slope is simply proportional to the depth of the lowest layer.) We will need to return to this point.

Phillips (1956) constructed the first "general circulation model," or "climate model," based on two-layer QG dynamics. Nowadays we might instead refer to this work as modeling the statistically steady state of a baroclinically unstable jet on a β -plane. Whatever we call it, this model still captures an impressive subset of the dynamics of the midlatitude storm tracks. Phenomena have been discovered in the solutions of these equations that have then been searched for and found in the atmosphere. The coherent baroclinic wave packets described in Lee and Held (1993) are an example from my own research. (Unfortunately, it is not obvious in reading that paper that we first encountered these wave packets while experimenting with the two-layer QG system.)

As long as the dissipative terms are linear, a theory for the time-mean geostrophic flow in this model reduces to a theory for the poleward eddy potential vorticity fluxes in the two layers, $\mathcal{P}_k \equiv \overline{v'_k q'_k}$, where an overbar refers to the zonal mean and a prime to deviations from this mean. We can relate these fluxes to the eddy momentum fluxes $\mathcal{M}_k \equiv \overline{v'_k u'_k}$ and the thickness (heat) fluxes $\mathcal{T}_k \equiv \overline{v'_k \eta'}$ (where $\mathcal{T}_1 = \mathcal{T}_2 \equiv \mathcal{T}$ from Margules' relation),

$$\mathcal{P}_1 = -\frac{\partial \mathcal{M}_1}{\partial y} + f\mathcal{T}/H; \quad \mathcal{P}_2 = -\frac{\partial \mathcal{M}_2}{\partial y} - f\mathcal{T}/H. \quad [1.2]$$

The two potential vorticity fluxes cannot fully determine the three fluxes (\mathcal{M}_1 , \mathcal{M}_2 , \mathcal{T}); therefore, the eddy thickness and momentum fluxes are more than we need to know if we are only interested in the mean zonal flow and the interface displacement (temperature).

The most fundamental limitation of QG dynamics is that it assumes a reference static stability; in this two-layer model the potential temperature difference between the two layers is fixed. One is perilously close to throwing the baby out with the bath water in such a theory. What could be more fundamental to a theory of climate than an understanding of the mean stratification of the atmosphere? But perhaps we can develop theories for the QG fluxes, and then use these outside of the QG framework to help as needed in determining the static stability. We illustrate this kind of argument below.

1.3. Eddy Closure in the Two-Layer Model

What is the scale of the typical energy-containing eddy in this two-layer QG model? Linear theory points to the radius of deformation, as it is the zonal scale of the most rapidly growing linear waves. A classic assumption (Stone 1972) is that the nonlinearity of the flow isotropizes the eddies in the horizontal and imprints this scale on the meridional as well as zonal eddy structure, and on eddy mixing lengths as well. An interesting implication is that there seems to be potential for scale separation in the horizontal, since this scale would then be independent of the mean flow inhomogeneity in the direction of the flux, in contrast to the situation in most laboratory turbulent flows.

If there is scale separation, one is justified in thinking in terms of local rather than global theories for the eddy fluxes. An example of a global theory is an approach referred to as *baroclinic adjustment*, in analogy with convective adjustment for gravitational instability (e.g., Stone 1978a). Since the instability of the flow can be thought of as due to the reversal in sign of the lower-layer potential vorticity gradient, suppose that the eddy fluxes are just sufficient to bring this gradient back to zero. Given a value of the radiative equilibrium shear and the width of the unstable region L_Q , the magnitude of the eddy potential vorticity flux required to destroy the gradient is proportional to L_Q^2 (since the rate of change of the mean gradient is proportional to the second derivative of the eddy flux). L_Q is a global piece of information. However, as L_Q is increased in numerical

simulations, the eddy potential vorticity fluxes are found to grow more slowly than L_Q^2 and eventually to asymptote to values independent of L_Q (Pavan and Held 1996). While baroclinic adjustment does not work in two-layer QG flows with large L_Q , it may very well be an adequate, indeed a very useful, approximation for the case of narrow regions of instability.

An example of a local theory is simple diffusion of potential vorticity, with a diffusivity determined by aspects of the local environment. We cannot expect a truly local diffusive theory to be exact. The relationship between eddy flux and environment must be nonlocal over the scale of the eddies at least. Additional nonlocality is introduced if the production and dissipation of the eddies are not colocated. For example, the simplest diffusive picture does not work when applied locally in longitude in the zonally asymmetric midlatitude storm tracks (Marshall and Shutts 1981; Illari and Marshall 1983). Eddies are preferentially generated in the strongly baroclinic zones at the jet entrance regions and decay downstream in the jet exit regions. It is only when one averages zonally over these regions of predominant eddy growth and eddy decay that one has a reason to expect a local, diffusive picture to hold in some approximate sense.

Given a diffusivity D and radiative relaxation time τ , we should not expect to reach the L_Q -independent asymptotic regime until $L_Q^2 > D\tau$, or $(L_Q/L)^2 > (\tau/T)$, where L and T are eddy length and time scales. The resulting scales are large compared to the radius of the Earth. But we do not need to be in this asymptotic regime to apply a diffusive theory; all that is required is scale separation $L_Q > L$. As in many applications of WKB-like theories, one can even hope that the local theory is adequate when $L_Q \approx L$.

The simplest scaling for the diffusivity is that suggested by Stone (1972): $D \sim VL \sim U\lambda$, where the eddy velocity scale V has been chosen proportional to the mean vertical shear U over the depth of the atmosphere. The assumption $V \sim U$ is equivalent to assuming that the eddy kinetic energy is proportional to the mean available potential energy (the increase in potential energy due to the interface slope) within a region of width λ . This diffusivity is itself proportional to the interface slope, or horizontal temperature gradient. If we can use this diffusivity for the sensible heat flux, following Stone, we obtain a heat flux proportional to the square of this gradient. Numerical experiments in the *homogeneous limit* described below clearly indicate that the eddy fluxes in this two-layer QG model are even more sensitive to the horizontal gradient; they also give us some guidance on how to incorporate β into the theory.

1.4. The Homogeneous Limit

Given the potential for a local theory, one is led to artificially create a truly homogeneous environment in which to study eddy fluxes in the simplest possible context. QG theory allows one to do this in an elegant way by assuming that there is a uniform zonal flow

in both layers, and, therefore, a uniform vertical shear and uniform potential vorticity gradients. One then assumes that the total flow consists of this environment, plus eddies constrained to be doubly periodic. One can think of this geometry as a generalization of the familiar QG β -plane to the case with potential vorticity gradients of opposite sign in the two layers.

In this geometry, the eddy fluxes are horizontally homogeneous. Therefore, according to (1.2), the potential vorticity fluxes reduce to the eddy thickness (heat) flux and are equal and opposite in the two layers. The momentum fluxes must also vanish if the climate is unique, since the equations are symmetric with respect to reflection in y , and the momentum fluxes change sign upon reflection. The central simplification is that one can study how the eddy fluxes are controlled by environmental parameters without simultaneously being concerned with the effect of these eddy fluxes on their environment.

A problem immediately arises from the inverse energy cascade, a cascade to larger rather than smaller scales. Calculations show unambiguously that the dominant eddy scale in the fully turbulent statistically steady state is generally larger than the radius of deformation due to this inverse cascade. It is useful to rearrange the two vertical degrees of freedom of this model into the barotropic ($\psi_1 + \psi_2$) and the baroclinic ($\psi_1 - \psi_2$) modes. The picture of the energy flows as a function of wavenumber in this modal basis has been described by Rhines (1977), Salmon (1978, 1980), and Larichev and Held (1995). The barotropic mode is energized by transfer from the baroclinic mode near the radius of deformation. The inverse cascade takes place in the barotropic mode, and energy is dissipated by surface friction on the scales to which this cascade carries the energy. If the cascade is extensive, the barotropic mode dominates the kinetic energy, so that the baroclinic potential vorticity (dominated on large scales by the thickness variations) can then be thought of as advected passively by the barotropic mode (since it does not induce the flow by which it is advected). The available potential energy, or thickness variance, is generated on these large energy-containing scales by extraction of energy from the environmental potential energy through downgradient thickness (heat) fluxes, just as in two-dimensional downgradient turbulent diffusion of a passive scalar, and cascades to smaller scales back towards the radius of deformation, completing the cycle.

Albeit directly applicable only for a rather special situation, it is striking how little this homogeneous turbulence picture has left in it that bears any resemblance to the scales and concepts familiar from linear theory.

As in Kolmogorov's classic work on the direct cascade of energy in three-dimensional turbulence, the key element of the two-dimensional inverse cascade, as described by Kraichnan (1971), is the rate of transfer of energy through the spectrum, ϵ . Together with the wavenumber k , ϵ determines the energy level of the flow and the characteristic time scale of the eddies. The key question is the scale at which the inverse energy cascade is halted.

At this point we take advantage of the insight of Rhines (1975) that the presence of an environmental barotropic vorticity gradient β can effectively stop the cascade, given the property of the Rossby wave dispersion relation that larger waves have larger intrinsic phase speeds (β/k^2). When these phase speeds become comparable to the characteristic velocity of the flow, the eddies morph into linear waves. Stopping the cascade in this way produces a flow that is simultaneously marginally turbulent and marginally wave-like, an elegant qualitative description of midlatitude eddies. From β and ϵ one forms length and time, or velocity, scales, or one can proceed directly to a diffusivity with units of length²/time,

$$D \sim \epsilon^{3/5} \beta^{-4/5}. \quad [1.3]$$

Surface friction must eventually remove energy from the model. In the presence of β , the flow forms zonal jets that store the energy until it is dissipated. Sensitivity of the diffusivity to the strength of surface friction might then modify this scaling to the extent that the structure of this jet reservoir feeds back on the eddy statistics. In the absence of β , the strength of surface friction must play a direct role in the scaling (Thompson and Young 2006), since it is then the only process that can stop the inverse cascade.

The potential energy extracted from the environment can be written in terms of the eddy potential vorticity flux in either layer,

$$\epsilon = \sum_i U_i \mathcal{P}_i = U \mathcal{P}_1 = -U \mathcal{P}_2 = U \beta D_1 (1 + \xi) = U \beta D_2 (\xi - 1), \quad [1.4]$$

where $U = U_1 - U_2$. We equate this production to the rate of energy transfer through the inverse energy cascade. We define a diffusivity in each layer as the eddy potential vorticity flux divided by the mean potential vorticity gradient. As $\beta \rightarrow 0$, $\xi \rightarrow \infty$, and $D_1 \rightarrow D_2$ (see Vallis 1988). Equating D in (1.3) with either D_1 or D_2 , in this limit we have

$$\epsilon = \frac{D}{T^2}, \quad T \equiv \frac{NH}{fU}, \quad [1.5]$$

where T^{-1} is often referred to as the Eady growth rate, though it does not enter here through any connection to linear theory. Combining with (1.3) one arrives at

$$D \sim \frac{1}{\beta^2 T^3} \quad [1.6]$$

or

$$\frac{D}{\beta \lambda^3} \sim \xi^3. \quad [1.7]$$

This is the scaling presented by Held and Larichev (1996). A more accurate fit to numerical experiments is provided by the modified formulation in Lapeyre and Held (2003), for which a satisfactory justification has yet to be provided. The proposal is simply to equate D with the lower-layer diffusivity D_2 , irrespective of the value of β .

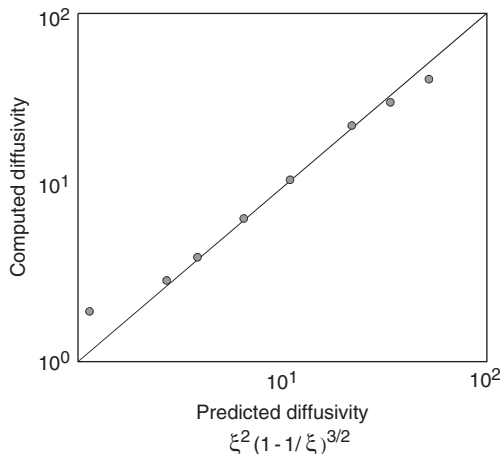


FIGURE 1.1. Comparing a theory for eddy heat fluxes in a homogeneous two-layer model with numerical simulations. Dots are the diffusivity, here non-dimensionalized by $U\lambda$, computed numerically in a 1024×1024 spectral simulation after Lapeyre and Held (2003), compared with the theoretical scaling provided by equation (1.8). The departures at large supercriticality are probably related to the finite size of the domain.

(I return to the motivation for this assumption in section 1.9.) The result is

$$\frac{D}{\beta\lambda^3} \sim \xi^3(1 - 1/\xi)^{3/2} \quad \text{or} \quad \frac{D}{U\lambda} \sim \xi^2(1 - 1/\xi)^{3/2} \quad [1.8]$$

This has the same $\xi \rightarrow \infty$ limit as (1.7). The fit to the numerical results, for fixed strength of surface friction, is shown in Fig. 1.1. This form also has the advantage that the diffusivity vanishes as $\xi \rightarrow 1$, consistent with the criterion for instability. This is my best shot at present for a qualitative explanation of the baroclinic eddy fluxes in this idealized homogeneous environment. As $\beta \rightarrow 0$ and $\xi \rightarrow \infty$, the eddy length scale increases without bound in this theory, implying that some other scales, determined by the surface friction or the domain geometry, must come into play.

Whether or not the details are right, this line of argument points to a flux that is very sensitive to environmental gradients: equation (1.7) yields a diffusivity proportional to the third power, a flux proportional to the fourth power, and an energy cycle ϵ proportional to the fifth power of the horizontal temperature gradient. Equation (1.8) only increases this sensitivity to ξ . In practice, this means that it is very hard, in this two-layer model, to change the gradient, to the extent that the system has difficulty supplying energy at the rate required.

As the width of the unstable region increases, the flow typically makes a transition from one to two and then to multiple jets, with a storm track associated with each jet. One is tempted to assume that the homogeneous limit cannot be relevant to the one-jet case, but only begins to become appropriate for the case of two or more jets, the former

being too inhomogeneous. The implication would be that the theory is irrelevant for the Earth, which has only one eddy-driven jet per hemisphere. An argument along similar lines starts with the observation that momentum fluxes vanish in the homogeneous system, averaged over space or, presumably, averaged over time at each point in space. But momentum fluxes appear to play a significant role in the stabilization of flows in the troposphere, as encapsulated in the *barotropic governor* mechanism of James (1987). The essence of this mechanism is that as barotropic shears are generated by the momentum fluxes, they progressively interfere with the baroclinic production mechanism and thereby limit growth.

My impression, in contrast, is that the equilibration mechanisms in one-jet and multiple-jet flows, and in this homogeneous model, are essentially the same, the dominant process being a generalized version of the barotropic governor, in which it is not only zonally averaged barotropic shears but the energy-containing barotropic mode, whether jet-like or not, that interferes with baroclinic production (see Salmon 1980). One does not need time-averaged momentum fluxes to create a barotropic governor; instantaneous shears are adequate.

On the other hand, the approach to the homogeneous limit is not likely to be simple. For example, Lee (1997) has shown that eddy statistics undergo non-monotonic evolution as one increases the width of the unstable region so as to make the transition from one jet to two. Relatively little has been achieved with regard to how one might use the homogeneous limit as a starting point for inhomogeneous theory. See in this regard Pavan and Held (1997).

1.5. Static Stability Maintenance

A key question in general circulation theory is whether or not the slope of the mean isentropes in the troposphere is strongly constrained. The observed slope is close to the aspect ratio of the troposphere: an isentropic surface that is near the ground in the Tropics rises to the tropopause in polar latitudes. Is this a coincidence, or is this particular slope favored?

Using the scaling from the previous section for the diffusivity due to baroclinic eddies, one can, in the spirit of Stone (1972), try to develop a theory for the static stability. In a stratified atmosphere, the expression (1.7) for the diffusivity, for example, implies that $D \sim \Delta_H^3 \Delta_V^{-3/2}$, where Δ_H and Δ_V are the horizontal and vertical potential temperature gradients, respectively. To obtain the horizontal eddy heat flux \mathcal{H} , one multiplies by another factor of Δ_H . To estimate the vertical eddy heat flux \mathcal{V} (ignored in QG theory) one can assume that the total flux is aligned along isentropic surfaces, averaged over the troposphere, so that $\mathcal{V} \Delta_V \sim \mathcal{H} \Delta_H$, or $\mathcal{V} \sim \Delta_H^5 \Delta_V^{-5/2}$. We next need to assume that the static stability is maintained by a balance between this eddy vertical heat flux and the destabilization by radiation. If we just assume that radiation relaxes Δ_V

to zero on some specified time scale, and that the vertical scale of the eddies is fixed, then $\Delta_V \sim \mathcal{V}$, resulting in the estimate $\Delta_V \sim \Delta_H^{10/7}$ and $D \sim \Delta_H^{6/7}$. The point of this manipulation is not to make a case for this specific result, but to illustrate how allowing the stability to adjust to changing eddy fluxes can potentially alter the sensitivity of the fluxes to the horizontal temperature gradient.

This scaling suggests that the isentropic slope can be altered by modifying the horizontal temperature gradient, albeit with some difficulty: $\Delta_H/\Delta_V \sim \Delta_H^{-3/7}$. If we use (1.8) instead of (1.7) the result is a much stronger constraint on the isentropic slope, when the system is in the proximity of the critical slope. But is this legitimate, given the seemingly artificial character of the two-layer model's critical slope?

As an alternative to thinking in two-layer terms, it has been suggested that one needs to couple the prediction of the static stability with a prediction of the tropopause height, and that by doing so one introduces a stronger constraint on the isentropic slope in the continuously stratified case (Held 1982). The essence of this argument can be understood by thinking of a continuously stratified QG model with fixed static stability and vertical shear; in this system the claim is that the distance that the eddy fluxes extend above the surface scales as $h \sim f^2 \partial U / \partial z / (\beta N^2)$, which is equivalent to $\xi \sim 1$. See Thuburn and Craig (1997) for a critique of this claim, and Schneider (2004) and Schneider and Walker (2006), who provide strong support for a refined version of this argument (while simultaneously calling into question the relevance of continuously stratified QG theory).

1.6. The Entropy Budget

In a comparison of theories for the poleward heat flux with various scaling arguments, Barry et al. (2002) combine the Rhines scale-inverse energy cascade relation (1.3) with an estimate of ϵ from a global entropy budget, rather than an energy budget. It is useful to understand how these approaches are related, as the entropy perspective may be especially useful in the presence of latent heat release.

Consider a dry atmosphere forced by the time-mean heating/cooling Q . The forcing decreases the entropy at a rate determined by averaging Q/T over the atmosphere. (From this point on, the symbol T refers to temperature, not to an eddy time scale.) This is a decrease in entropy because Q creates temperature gradients by warming (cooling) regions that are already relatively warm (cool). In a steady state this entropy destruction is balanced by production due to irreversible processes, the dominant one in a dry atmosphere being the dissipation of kinetic energy (that is, the diffusion of momentum), the rate of kinetic energy dissipation being ϵ once again. We ignore radiative damping of transients due to the correlation in time between Q and T , which will create entropy, and we also ignore diffusion of temperature. The latter tends to be small because temperature, in balanced flows, cascades to small scales only at the surface

and not in the interior of the troposphere. Therefore,

$$-\int \frac{Q}{T} \approx \frac{\epsilon}{T_\epsilon}, \quad [1.9]$$

where T_ϵ is the average temperature at which the energy dissipation occurs and all integrations are over the mass of the atmosphere. We assume small departures of T and T_ϵ from a reference temperature T_0 as needed.

Barry et al. (2002) estimate ϵ in their model by taking the distribution of Q as given. This may seem like one is giving oneself too much information, in that Q is dominated by the divergence of the eddy heat flux for which one is trying to develop a theory. But suppose one has a theory for the eddy diffusivity, and eddy heat or potential vorticity fluxes, that depends on ϵ . Given ϵ , one determines the fluxes and temperatures, and therefore Q ; one can then iterate to obtain self-consistency. A difficulty with this approach is that one loses the sense of a local theory, ϵ being determined by a global integral.

But one can regain a local perspective by setting $Q = \nabla \cdot F$, where F is the flux of dry static energy, and then integrating by parts:

$$-\frac{\epsilon}{T_\epsilon} \approx \int \frac{1}{T^2} F \cdot \nabla T = \int \frac{1}{T} F \cdot \nabla \ln T = \int \frac{1}{T} F_H \frac{\partial \ln T}{\partial y} \Big|_M. \quad [1.10]$$

In the final expression, we have assumed that the climate is zonally symmetric, so that F is a vector in the $y - z$ (or $y - p$) plane with horizontal component F_H , and have let M denote a coordinate that is constant on the surface along which F is aligned. One can now apply this locally, setting the local ϵ -density equal to the integrand. To see the connection with the QG arguments above, one needs to assume that $M \approx \theta$. Letting S be the isentropic slope,

$$F_H \frac{\partial \ln T}{\partial y} \Big|_\theta = F_H \frac{R}{c_p} \frac{\partial \ln p}{\partial y} \Big|_\theta = F_H \frac{R}{c_p} S \frac{\partial \ln p}{\partial z} = F_H \frac{g}{c_p T} S. \quad [1.11]$$

Substituting for $F_H \approx c_p \overline{v'T'}$ and setting

$$S = -\frac{\partial_y \theta}{\partial_z \theta} \quad [1.12]$$

and $(g/T)\overline{v'T'} = Df\partial_z U$, we regain equation (1.5). For later reference, notice that the static stability makes its only appearance in this argument at the point when the mixing slope is set equal to the isentropic slope.

Entropy and available potential energy budgets are not equivalent in general, but they are closely enough related that they lead to essentially the same scaling approximations.

1.7. Moist Eddies

We would like our theories for midlatitude eddy fluxes to help us understand the implications of the increase in moisture content in the atmosphere that will accompany global warming. We would also like to make use of the seasonal cycle to test our theories for these eddy fluxes (e.g., Stone and Miller 1980), but these tests are not very convincing as long as one is ignoring the effects of latent heat release, which vary seasonally in tandem with the variations in the large-scale temperature gradients. The length scale of midlatitude eddies is observed to be larger in northern winter than in summer. Is this due to the larger eddy energies in winter, which result in a larger Rhines scale, or is it that eddies are smaller in summer because of a reduction in an *effective static stability* due to latent heat release? A central theoretical issue is whether there are ways of using concepts like moist entropy (Emanuel and Bister 1996) or moist available potential energy (Lorenz 1978) so as to carry some of the lines of argument developed for dry eddies over to the moist case.

Lapeyre and Held (2004) construct a relatively simple moist model by adding a water vapor variable to the two-layer QG model. To obtain consistent energetics, they treat moisture in an analogous way to temperature (or thickness) by requiring the moisture field to be a small perturbation away from a prescribed mean value that is uniform within each layer. Despite this limitation, the form of this model's energetics is of interest. Here I provide a brief sketch of QG moist energetics more generally, because it has a feature that is counterintuitive (for me) and may have interesting implications for how we think about moist eddies.

In a dry QG model the available potential energy (APE) is proportional to the variance of the interface displacement. This form follows from the QG thermodynamic equation of the form

$$\frac{\partial b}{\partial t} = -N^2 w - J(\psi, b). \quad [1.13]$$

We use the Boussinesq approximation for simplicity, with b the buoyancy; the final term represents horizontal advection by the geostrophic flow. The conversion of potential to kinetic energy is $[bw]$, where brackets denote a global mean. One manipulates the buoyancy equation to have the same expression on the right-hand side by multiplying by b/N^2 and averaging:

$$\frac{\partial \text{APE}}{\partial t} = -[wb]; \quad \text{APE} \equiv \left[\frac{b^2}{2N^2} \right]. \quad [1.14]$$

In a moist QG model, one has instead, schematically,

$$\frac{\partial b}{\partial t} = -N^2 w - J(\psi, b) + LP, \quad [1.15]$$

where P is the condensation rate and L the latent heat, and

$$\frac{\partial q}{\partial t} = -(\partial_z Q)w - J(\psi, q) - P, \quad [1.16]$$

where q is now the moisture perturbation (not potential vorticity) and $Q = Q(z)$ the reference moisture. Forming an equation for the buoyancy variance results in the term $[Pb]$ on the right-hand side, which we wish to avoid. One can eliminate P by forming a moist enthalpy equation for $h \equiv b + Lq$, but forming an equation for the variance of h generates a term proportional to $[hw]$ rather than $[bw]$. One can try to remedy this problem by forming an equation for the variance of the moisture, but this reintroduces the precipitation on the right-hand side through $[qP]$. The successful manipulation uses the variance of the saturation deficit, $d = q_s - q$, where one assumes that precipitation occurs when saturation occurs, so that $[dP] = 0$. Here I describe the simplest case, in which q_s is a constant, independent of temperature (the case in which the saturation vapor pressure is a function of temperature or buoyancy (b) is a bit more involved). We can then set this $q_s = 0$ (recall that q is here the departure from the reference $Q(z)$). We finally obtain an equation of the form

$$\frac{\partial \text{QAPE}}{\partial t} = -[wb]; \quad \text{QAPE} \equiv \frac{1}{2} \left[\frac{h^2}{(N^2 - L|\partial_z Q|)} + L \frac{d^2}{|\partial_z Q|} \right]. \quad [1.17]$$

Thus, our moist available potential energy (QAPE) has one term proportional to the variance of the moist enthalpy, divided by a moist stability, plus an additional term proportional to the variance of the saturation deficit, or dew point depression. This form is presumably related to Lorenz's general form for moist APE, specialized to the case of small interface displacements and small moisture deficits. The implications for moist energetics of the presence of the term proportional to the saturation deficit variance are obscure but intriguing. *There is an energetic cost to an increase in undersaturation.* I find it difficult to understand this statement intuitively. See Frierson et al. (2004) for an application of an analogous expression to a shallow-water model.

The sources/sinks of QAPE also have additional terms not present in the dry case. Evaporation into unsaturated air and diffusion of water are both important sinks of QAPE and have no direct counterparts in the dry case. Unlike temperature, the water mixing ratio does cascade to small scales in this QG flow, so the diffusive loss of mixing-ratio variance is both significant and energetically important from the perspective of QAPE. There is an intriguing resemblance between these sinks of QAPE and the sources of irreversibility in a moist entropy budget. As discussed by Emanuel and Bister (1996) and Pauluis and Held (2002) for tropical convection, the efficiency of the kinetic energy cycle is reduced by diffusion of moisture, either due to a cascade of variance to small scales, or to evaporation into unsaturated air (microscopically, the latter is simply diffusion down the gradient between the saturated air in contact with

the liquid and the air a bit further removed). Equation (1.9) is replaced by

$$\frac{\epsilon}{T_\epsilon} \approx - \int \frac{Q}{T} - R, \quad [1.18]$$

where R is the positive definite generation of entropy due to diffusion of vapor, and Q now includes radiative cooling and surface evaporation plus surface sensible heating (but not latent heat release!). It is likely that the term R reduces the efficiency of midlatitude eddy dynamics substantially (especially in summer) just as it does the efficiency of tropical convection.

How would latent heat release modify the kinds of scaling arguments described earlier? We can try to work from either a moist available potential energy or a moist entropy perspective, but the latter may be simpler, especially since the QG version of QAPE is undoubtedly too restrictive. Setting Q equal to the divergence of the eddy moist static energy flux, F , with horizontal component F_H equal to the flux of moist enthalpy $\overline{v'h'} = c_p \overline{v'T'} + L \overline{v'q'}$, we can write

$$\frac{\epsilon}{T_\epsilon} = \int \overline{v'h'} \frac{1}{T} \left. \frac{\partial \ln(T)}{\partial y} \right|_M - R, \quad [1.19]$$

where the derivative is taken along the mixing surface, defined by the direction of the eddy moist static energy flux. One can then diffuse moist enthalpy down the mean moist enthalpy gradient, and combine this expression with (1.3) or its equivalent. Thus, moisture and latent heat release affect the theory of Held and Larichev (1996) or Barry et al. (2002) in three ways: by reducing efficiency through the term R , by increasing the mixing slope (i.e., reducing the effective static stability), and by replacing the dry enthalpy by the moist enthalpy as the quantity being diffused. Without expressions for the mixing slope and the efficiency reduction, this is not a closed theory, but it gives us some feeling for what such a theory might look like.

1.8. An Idealized Moist Model on the Sphere

Does latent heat release reduce the mean length scale of the energy-containing eddies? The Eady model linear theory of Emanuel et al. (1987) indicates potential for a reduction by a factor of 2 or so. But if one thinks in terms of the Rhines scale, one might guess that a reduction in effective static stability likely increases the scale by increasing the eddy kinetic energy.

Frierson et al. (2006, hereafter FHZ) have constructed an idealized moist general circulation model (GCM) on the sphere in part to address questions of this kind. The moist general circulation is generally addressed with comprehensive atmospheric climate models in which clouds, convection, and radiative transfer interact in a host of subtle ways that are only dimly appreciated, and in which there are sensitivities to resolution, time-stepping, and (often undocumented) details in the closure schemes

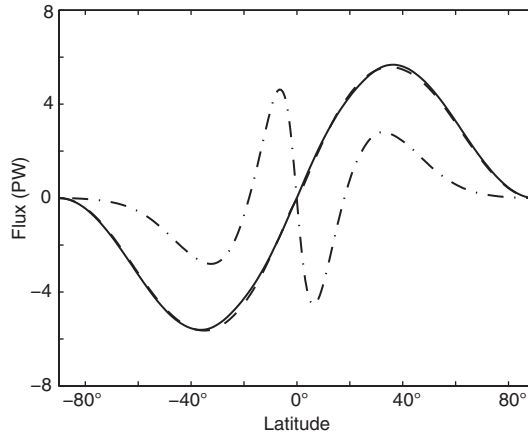


FIGURE 1.2. Poleward energy fluxes in moist and dry idealized models. Solid: total energy flux in moist model; dashed: dry static energy flux (and, therefore, total flux) in dry model; dash-dot: latent heat flux in moist model. (Provided by D. Frierson.)

that makes it difficult to reproduce model results. In FHZ, the radiation is a function of temperature only, there is no condensate, and the boundary layer and convective closures are kept simple enough to encourage tests of reproducibility and sensitivity to resolution. In the simplest case, the model is run with large-scale condensation only, with no convective closure scheme.

The initial results with the FHZ model show surprising insensitivity of the eddy scale to the amount of moisture in the atmosphere, and, therefore, to the amount of latent heat release. There is essentially no difference in the midlatitude eddy spectrum between the dry limit of this model and a control run with realistic moisture content. The dry static stability increases with increasing moisture to prevent large changes in moist stability, so the constancy of the eddy length scale is in disagreement with any theory based on an effective stability that scales with the dry stability. The Rhines scale, on the other hand, does predict the constancy of this scale as the moisture increases if, it turns out, one allows oneself to compute it at the position of the maximum eddy kinetic energy (FHZ). This latitude moves polewards as moisture increases, and the Rhines scale remains unchanged only because of the canceling effects of a reduction in eddy energy and a reduction in β . But this does not explain whether the cancellation is a coincidence or a result of some dynamical constraint.

The results in FHZ are also intriguing with respect to the question of the partitioning of the poleward heat flux between latent and sensible parts. As shown in Fig. 1.2, the total poleward flux in this model stays remarkably constant (to within 1%) as the amount of water vapor, and the poleward flux of latent energy, increases from the dry limit to a realistic value. A reduction in sensible flux cancels the increase in latent flux. It is sometimes argued (following Stone 1978b) that the total atmospheric

flux is more or less as large as it can possibly be, since the profile of outgoing infrared flux is much flatter than that of the absorbed solar flux. But analysis shows that there is substantial room for an increase in the FHZ model. In any case, why should the atmosphere be incapable of reversing the sign of the outgoing longwave gradient? It is not difficult to construct a model that does precisely this (D. Frierson, personal communication).

I have recently examined this compensation in the comprehensive climate model when run in aqua-planet mode (over a uniform boundary condition of slab ocean with fixed heat capacity) of the Geophysical Fluid Dynamics Laboratory (GFDL) and find about 80%, rather than near perfect, compensation when the atmospheric CO₂ is doubled. My impression is that this level of compensation is typical in comprehensive climate models (e.g., Manabe and Bryan 1985). We suspect that the key to the near-perfect cancellation in FHZ is the fact that the radiation is a function of temperature only.

A final question that is addressed by the FHZ model is that of the role of latent heating, and moist convection more specifically, in maintaining the static stability in midlatitudes. The claim is that this idealized model supports the picture of Jukes (2000), who argues that the large-scale eddy fluxes are not capable of stabilizing the atmosphere to the point of preventing moist convection in the warm sectors of extratropical cyclones. A possible implication is that the mean static stability of the extratropical troposphere is maintained by this moist convection so that the favorable sectors of extratropical cyclones are moist neutral. The average moist stability of the atmosphere is then determined by the difference between the average boundary-layer moist enthalpy and the maximum value of this boundary-layer moist enthalpy within the eddies, or equivalently by the rms moist enthalpy in the boundary layer. The latter, in turn, is presumably determined by the large-scale eddy mixing length and the horizontal mean moist enthalpy gradient.

Clearly, we have just scratched the surface of many central climatic questions involving the effects of moisture on the large-scale circulation, many of which are important in understanding global warming simulations. Idealized models of the moist general circulation are sorely needed to make contact with our even-more idealized dry models and with the high-end comprehensive models that play the predominant role when we apply climate models to real-world problems.

1.9. Upper vs. Lower Tropospheric Dynamics

There is an important qualitative distinction between the upper and lower troposphere that impacts the general circulation in numerous ways: the upper troposphere is more wave-like than the lower troposphere. This distinction must fundamentally be due to β , the environmental vorticity gradient. In the two-layer model, for example, β adds to

the contribution of vertical shear to the upper-layer potential vorticity gradient, while it tends to cancel this contribution in the lower layer. The result is that potential vorticity gradients are larger in magnitude in the upper than in the lower layer. These gradients create the restoring forces for Rossby waves. A disturbance of a given scale will propagate westward with respect to the upper-level flow more strongly than it will propagate eastward with respect to the lower-level flow (in the lower layer the potential vorticity gradient is negative, causing Rossby waves to propagate eastward rather than westward.) As one consequence, β pushes the steering level for baroclinic instabilities, where the phase speed matches the environmental flow, into the lower troposphere.

When waves on shear flows grow, they typically break when the flow perturbations u' become comparable to $\bar{u} - c$, the phase speed of the wave with respect to the environment. So eddies of the same amplitude will break first in the lower layer, and the upper layer will remain more linear. To the extent that they are determined by this kind of breaking criterion, eddy amplitudes should be larger in the upper than in the lower layer. The flow in each layer can be thought of as induced by the potential vorticity in both layers, but if the eddy amplitudes are larger aloft, the lower-layer flow will be primarily induced by the potential vorticity in the upper layer, while the upper-layer flow will be primarily self-induced, allowing more wave-like evolution. I suspect that this has something to do with the fact that the two-layer closure theory works best when based on lower-layer diffusion of potential vorticity, leading to equation (1.8).

The distinction between upper- and lower-troposphere dynamics, with the latter more turbulent and the former more wave-like, is central to any discussion of eddy momentum fluxes. *That the eddy momentum fluxes are almost entirely confined to the upper troposphere is a consequence of this distinction.* Rossby waves propagating away from their midlatitude source on a positive potential vorticity gradient (as in the upper layer of a two-layer model) converge eastward (positive) angular momentum into midlatitudes; Rossby waves propagating on a negative vorticity gradient (as in the lower layer of the two-layer model) converge negative momentum into the source latitudes. Because almost all of the propagation in fact occurs in the upper troposphere, surface westerlies are generated in midlatitudes to remove the positive momentum flux convergence. If lower-tropospheric propagation were dominant, surface easterlies would be generated in midlatitudes. All of the profound consequences for the atmosphere and the oceans that follow from the existence of midlatitude surface westerlies result from this asymmetry between upper and lower tropospheres.

The simplest picture of linear midlatitude eddies in the upper troposphere starts with a barotropic westerly point jet, $u(y) = -\Delta|y|$, the corresponding vorticity distribution being a single contour separating two homogenized regions, with jump $\Delta = 2\Lambda$ across the contour. This flow supports the simplest Rossby edge waves with dispersion relation $c = U - \Delta/(2k)$. One can usefully speak of a *capacity* of this jet, the amplitude of the waves that can propagate along this contour without significant breaking. Using the criterion $u' \sim \bar{u} - c$ for overturning streamlines in the frame of

reference of the wave, one gets $u' \sim \Delta/k$. The corresponding trajectory displacements are also of the order of the inverse wavenumber k^{-1} . If we now think of the homogenized regions on each side of this contour, and, therefore, the size of the jump Δ , as having been created by the eddies themselves from the environmental gradient β , we are led to assume that $\Delta \sim \beta k^{-1} = \beta L$, or $u' \sim \beta L^2$. The resulting relation between the eddy scale and eddy energy is just that proposed by Rhines, even though there is no association here with an inverse cascade. This picture may help us understand why it is the Rhines scale *at the latitude of the jet* that seems to be the relevant scale for the eddies in FHZ.

The homogeneous turbulence theory outlined above can be thought of as consisting of three relations between three unknowns: the strength of the energy generation/dissipation ϵ , an eddy length scale L , and an eddy velocity scale V (or a diffusivity VL). The three relations are (1) an entropy or available potential energy budget that relates ϵ and D , (2) the Rhines scale relation between V and L , and (3) the turbulent cascade scaling $\epsilon \approx V^3/L$. (One can combine (2) and (3) to give equation (1.3).) In light of the results described by Schneider (2004) for a primitive-equation model on the sphere in which the static stability adjusts to prevent a significant inverse cascade, it may be desirable to try to retain (1) and (2), but to replace (3) with a non-turbulent alternative, a choice made palatable by this alternative argument for the Rhines scale.

A picture that emerges is of an upper-level waveguide fed by baroclinic eddy production, with an eddy sink given by the sloughing off of excess wave activity and fed by baroclinic eddy production that is, in turn, determined by the diffusion of low-level PV (or heat) controlled by the upper-level eddy amplitudes. One can try to expand this picture into a theory for the zonally asymmetric storm tracks (see in this regard Swanson et al. [1997] and chapter 4 in this volume) in which the key new ingredient is the zonally varying capacity of the jet.

While we have some useful pictures of upper-level dynamics that help us understand the eddy momentum fluxes, and even some simple linear models that fit the eddy momentum fluxes quantitatively, given the low-level eddy stirring (DelSole 2001), our understanding of the location of the surface westerlies is far from complete. This is evident when we perturb the system and try to understand how and why the surface westerlies (and the associated eddy momentum flux convergence) move. An excellent example is provided by experiments in which the strength of the surface friction is modified; as the friction is weakened, the westerlies move poleward (Robinson 1997). Figure 1.3 is from unpublished work by G. Chen (personal communication, 2005), using the dry dynamical core benchmark of Held and Suarez (1994). The theory for this shift is still undeveloped. Robinson has suggested that a barotropic governor mechanism is the key: as the surface friction is reduced, surface winds and horizontal shears increase, and, it is argued, the resulting stabilization by these shears is larger on the equatorward side. How one would go about making this hypothesis quantitative and then testing it remains a challenge.

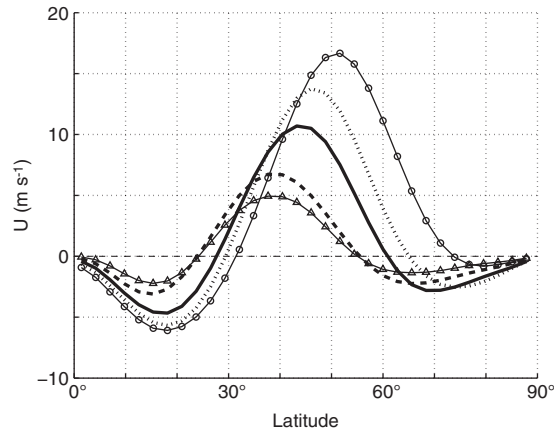


FIGURE 1.3. The near-surface zonal-mean wind field in the climate of an idealized dry general circulation model (GCM) for several values of the strength of the surface friction. The surface friction is a linear drag in the lower troposphere, with different relaxation times (0.5, 0.75, 1, 1.25, 1.5 days) in the different cases. The longer relaxation times produce stronger winds and a poleward displacement of the westerlies. (Provided by G. Chen.)

Poleward displacement of the surface westerlies and storm tracks is also seen in global warming simulations. Several alternative explanations have been offered for this shift, some involving the increase in latent heat release. It will be a challenge to our theories, and our ability to develop the appropriate hierarchy of idealized models, to cleanly isolate the dynamics underlying this shift.

Acknowledgments

I thank Dargan Frierson, Pablo Zurita-Gotor, and Gang Chen for their insights and help with the figures.

References

- Barry, L., G. C. Craig, and J. Thuburn, 2002: Poleward heat transport by the atmospheric heat engine. *Nature*, **415**, 774–777.
- DelSole, T., 2001: A simple model for transient eddy momentum fluxes in the upper troposphere. *J. Atmos. Sci.*, **58**, 3019–3035.
- Emanuel, K. A., and M. Bister, 1996: Moist convective velocity and buoyancy scales. *J. Atmos. Sci.*, **53**, 3276–3285.

- Emanuel, K. A., M. Fantini, and A. J. Thorpe, 1987: Baroclinic instability in an environment of small stability to slantwise moist convection. Part I: Two-dimensional models. *J. Atmos. Sci.*, **44**, 1559–1573.
- Frierson, D. M. W., A. J. Majda, and O. M. Pauluis, 2004: Large scale dynamics of precipitation fronts in the tropical atmosphere: A novel relaxation limit. *Commun. Math. Sci.*, **2**, 591–626.
- Frierson, D. M. W., I. M. Held, and P. Zurita-Gator, 2006: A gray radiation, aquaplanet moist GCM: Part 1: Static stability and eddy scale. Submitted to *J. Atmos. Sci.*
- Held, I. M., 1982: On the height of the tropopause and the static stability of the troposphere. *J. Atmos. Sci.*, **39**, 412–417.
- Held, I. M., 2005: The gap between simulation and understanding in climate modeling. *Bull. Amer. Meteor. Soc.*, **86**, 1609–1614.
- Held, I. M., and V. D. Larichev, 1996: A scaling theory for horizontally homogeneous, baroclinically unstable flow on a beta plane. *J. Atmos. Sci.*, **53**, 946–952.
- Held, I. M., and M. J. Suarez, 1994: A proposal for the intercomparison of the dynamical cores of atmospheric general circulation models. *Bull. Amer. Meteor. Soc.*, **75**, 1825–1830.
- Illari, L., and J. C. Marshall, 1983: On the interpretation of eddy fluxes during a blocking episode. *J. Atmos. Sci.*, **40**, 2232–2242.
- James, I. N., 1987: The suppression of baroclinic instability in horizontally sheared flows. *J. Atmos. Sci.*, **44**, 3710–3720.
- Juckes, M. N., 2000: The static stability of the midlatitude troposphere: The relevance of moisture. *J. Atmos. Sci.*, **57**, 3050–3057.
- Kraichnan, R. H., 1971: Inertial range transfer in two and three dimensional turbulence. *J. Fluid Mech.*, **47**, 525–535.
- Larichev, V. D., and I. M. Held, 1995: Eddy amplitudes and fluxes in a homogeneous model of fully developed baroclinic instability. *J. Phys. Oceanogr.*, **25**, 2285–2297.
- Lapeyre, G., and I. M. Held, 2003: Diffusivity, kinetic energy dissipation, and closure theories for the poleward eddy heat flux. *J. Atmos. Sci.*, **60**, 2907–2916.
- Lapeyre, G., and I. M. Held, 2004: The role of moisture in the dynamics and energetics of turbulent baroclinic eddies. *J. Atmos. Sci.*, **61**, 1693–1710.
- Lee, S., 1997: Maintenance of multiple jets in a baroclinic flow. *J. Atmos. Sci.*, **54**, 1726–1738.
- Lee, S., and I. M. Held, 1993: Baroclinic wave packets in models and observations. *J. Atmos. Sci.*, **50**, 1413–1428.
- Lorenz, E. N., 1978: Available energy and the maintenance of a moist atmosphere. *Tellus*, **30**, 15–31.
- Manabe, S., and K. Bryan Jr., 1985: CO₂-induced change in a coupled ocean-atmosphere model and its paleoclimatic implication. *J. Geophys. Res.*, **90(C6)**, 11,689–11,707.
- Marshall, J. C., and G. L. Shutts, 1981: A note on rotational and divergent eddy fluxes. *J. Phys. Oceanogr.*, **11**, 1677–1680.
- Pauluis, O., and I. M. Held, 2002: Entropy budget of an atmosphere in radiative-convective equilibrium. Part II: Latent heat transport and moisture processes. *J. Atmos. Sci.*, **59**, 140–149.
- Pavan, V., and I. M. Held, 1996: The diffusive approximation for eddy fluxes in baroclinically unstable jets. *J. Atmos. Sci.*, **53**, 1262–1272.
- Phillips, N., 1956: The general circulation of the atmosphere: a numerical experiment. *Quart. J. Roy. Meteor. Soc.*, **82**, 123–164.
- Rhines, P. B., 1975: Waves and turbulence on a β -plane. *J. Fluid Mech.*, **69**, 417–443.
- Rhines, P. B., 1977: The dynamics of unsteady currents. In *The Sea*, Vol. 6, E. A. Goldberg, I. N. McCane, J. J. O'Brien, and J. H. Steele, Eds., Wiley, 189–318.

- Robinson, W. A., 1997: Dissipation dependence of the jet latitude. *J. Climate*, **10**, 176–182.
- Salmon, R. S., 1978: Two-layer quasi-geostrophic turbulence in a simple special case. *Geophys. Astrophys. Fluid Dyn.*, **10**, 25–52.
- Salmon, R. S., 1980: Baroclinic instability and geostrophic turbulence. *Geophys. Astrophys. Fluid Dyn.*, **15**, 167–211.
- Schneider, T., 2004: The tropopause and the thermal stratification in the extratropics of a dry atmosphere. *J. Atmos. Sci.*, **61**, 1317–1340.
- Schneider, T., and C. C. Walker, 2006: Self-organization of atmospheric macroturbulence into critical states of weak nonlinear eddy-eddy interactions. *J. Atmos. Sci.*, **63**, 1569–1586.
- Stone, P. H., 1972: A simplified radiative-dynamical model for the static stability of rotating atmospheres. *J. Atmos. Sci.*, **29**, 405–418.
- Stone, P. H., 1978a: Baroclinic adjustment. *J. Atmos. Sci.*, **35**, 561–571.
- Stone, P. H., 1978b: Constraints on dynamical transport of energy on a spherical planet. *Dyn. Atm. And Ocean.*, **2**, 123–139.
- Stone, P. H., and D. A. Miller, 1980: Empirical relations between seasonal changes in meridional temperature gradients and meridional fluxes of heat. *J. Atmos. Sci.*, **37**, 1708–1721.
- Swanson, K. L., P. J. Kushner, and I. M. Held, 1997: Dynamics of barotropic storm tracks. *J. Atmos. Sci.*, **54**, 791–810.
- Thompson, A. F., and W. R. Young, 2006: Scaling Baroclinic Eddy Fluxes: Vortices and Energy Balance. *J. Phys. Oceanogr.*, **36**, 720–738.
- Thuburn, J., and G. C. Craig, 1997: GCM tests of theories for the height of the tropopause. *J. Atmos. Sci.*, **54**, 869–882.
- Vallis, G. K., 1988: Numerical studies of eddy transport properties in eddy-resolving and parameterized models. *Quart. J. Roy. Meteor. Soc.*, **114**, 183–204.

Index

- Abrupt climate change
atmospheric circulation regimes, heat transport and, 350–51
Caribbean, Tropical Atlantic, Africa and, 336–37, 342
deep ocean circulation and, 339–40
ENSO and, 353–55
global mean climate and, 339
lack of modern analogues to, 342–43
northern extratropics and, 337–38
ocean, atmosphere heat transport and, 361
overview of, 331–33, 362–64
polar ice cores and, 333–35
seasonality around North Atlantic Ocean, 340–41, 349–50
Southern Hemisphere and, 338–39
spatial character of, 343
summer climate and, 352–53
surface Atlantic Ocean and, 335–36
thermohaline circulation and, 343–49
tropical climate reorganization and, 360–61
tropical forcing of, 353
tropical heating, extratropical jets, storm tracks and, 355–60
winter shift to zonal circulation and, 351–52
- Adiabatic lapse rate, 53, 70, 189, 191, 195–97, 199–200
- Advection-condensation model, 154
- African Humid Period, 332–33
- Ageostrophic mass flux, 61–62
- Albedo
abrupt climate change and, 339
ice feedback, 147, 150–51
northern African summer monsoon and, 282
thermal stratification and, 50
- Alkenones, 335–36, 364–65
- Almost intransitive systems, 335
- Angular momentum, 54–55, 220, 252, 255
- Annular modes, 110, 134–37
- Anomalous gross moist stability mechanism, 294, 295
- Antarctica, 332, 333–35
- Arakawa-Schubert convection scheme, 190–91
- Atlantic Ocean, 335–37, 342. *See also* North Atlantic Ocean
- Atmospheric circulation regimes, abrupt climate change and, 350–51
- Atmospheric general circulation models (AGCMs)
cloud biases and, 308–11
Madden-Julian Oscillation (MJO) bias and, 307
superparameterization and, 315–16
warm eastern ocean/double ITCZ bias and, 303–5
- Available potential energy, moist eddies and, 12–13
- Back pressure effect, 224–25
- Back trajectories, 156–58, 164, 175–78
- Background flow, storm track dynamics and, 89–90
- Baroclinic adjustment

- boundary layers and, 33–37
- Charney problem and, 33
- eddy lifecycles and, 37–40
- forcing, dissipation and, 40–42
- overview of, 25–28
- quasigeostrophic constraints on, 70–71, 74
- temperature gradients and, 22, 23–24
- two-layer QG model and, 4–5, 28–33
- Baroclinic eddy fluxes
 - circulation background state and, 110
 - Eliassen-Palm fluxes and, 138
 - equatorial superrotation and, 131
 - jet and storm track shifts and, 125–27
 - potential vorticity and, 111–19
 - thermal stratification and, 49, 55–59, 72
 - tropical warming and, 120, 128
 - vertical extent of, 65–67
- Baroclinic zones, storm tracks and, 79, 85–86, 88–89
- Barotropic governor mechanism, 9, 18
- Barotropic jets, 17–18
- Bermuda Rise, 335–36
- Beta-plume, 257
- Bølling-Allerød warm period, 331, 335–37, 339–40, 349, 360
- Boundary layer. *See also* Planetary boundary layer (PBL)
 - baroclinic adjustment and, 26, 29–30, 33–37, 40–41
 - potential vorticity gradients and, 34–35
 - quasi-equilibrium and, 231
 - troposphere as, 48
- Boussinesq approximation, 12, 38
- British Isles, 337, 340, 349
- Brunt-Väisälä frequency, 79
- Bulk moist stability. *See* Gross moist stability
- Buoyancy flux, 13, 188

- Capacity of barotropic jets, 17–18
- Carbon dioxide, 147, 148–49, 181
- Cariaco Basin, 336–37, 339, 345
- Caribbean, 336–37, 340
- Charney problem, 33, 38
- Charney-Stern condition for instability, 29–31
- Circulation constraint, 253–57, 257–61
- Cirrostratus/cirrocumulus (CsCc), 285–87
- Clausius-Clapeyron relation, 145, 153, 159, 180
- Climate change. *See* Abrupt climate change; Global warming
- Cloud radiative forcing, defined, 308
- Cloud-resolving cumulus parameterization. *See* Superparameterization
- Cloud-resolving models (CRMs)
 - AGCM response to climate warming and, 318
 - cloud-climate feedback uncertainties and, 317–18
 - DARE climate sensitivity results and, 324–26
 - feedbacks in CRM simulations and, 318–24
 - global climate dynamics and, 314–17
 - modeling and, 302–3, 326
 - tropical biases and, 311–14
- Clouds
 - CISK and, 221
 - convection, precipitation and, 285–87
 - effect of biases in on modeling, 308–11
 - effective static stability and, 285–87
 - radiative effects of, 182, 205–6, 214, 291
 - surface flux mechanisms and, 293
 - thermal stratification and, 50
 - trajectory approach and, 158
 - water vapor-radiation interactions and, 205–6
- Clouds and the Earth's Radiant Energy System (CERES), 308, 311
- Cold trap, 162–163, 171–72
- Column radiation model, 49
- Condensation, 145, 154, 159–63
- Conditional instability of the second kind (CISK), 221, 228
- Convection, 53–55, 71, 74, 187–90, 207–10. *See also* Deep ocean circulation
- Convective adjustment, 24–25
- Convective available potential energy (CAPE)
 - Madden-Julian Oscillation (MJO) bias and, 307
 - PBL convergence and, 245
 - precipitation and, 230–31
 - quasi-equilibrium and, 191
 - tropical biases and, 311

- Convective inhibition (CIN), 231, 245
- Convective quasi-equilibrium. *See also* Quasi-equilibrium tropical circulation model (QTCM)
- gross moist stability and, 278–79
 - moist static energy budget and, 280–81
 - moist teleconnection and, 289
 - overview of, 267–68
- Convergence. *See also* Intertropical convergence zone (ITCZ); Moisture convergence
- CISK arguments and, 228
 - convective available potential energy (CAPE) and, 245–46
 - East Pacific Investigation of the Climate (EPIC) and, 239
 - Lindzen-Nigam model and, 224
 - momentum fluxes and, 117, 229
 - precipitation and, 220
 - vertical shear and, 39
- Coupled ocean-atmosphere general circulation models (CGCMs), 303–5, 306, 326
- Coupling
- abrupt climate change and, 360–61
 - atmospheric circulation regimes, heat transports and, 350–51
 - global climate dynamics and, 361–62
 - monsoons, deserts and, 333
 - North Atlantic climate change and, 349–50
 - oceans and, 206–7
 - summer climate and, 352–53
 - tropical circulation and, 353–60
 - tropical climate reorganization and, 360–61
 - warm eastern ocean/double ITCZ bias and, 303–5
 - winter shift to zonal circulation and, 351–52
- Critical slope of isentropes, 3
- Cyclones, 55, 204, 210–13, 230. *See also* Storm tracks
- Dansgaard-Oeschger Event, 360
- Deep ocean circulation
- abrupt climate change and, 333, 339–40, 361–62
 - convective available potential energy (CAPE) and, 230
 - North Atlantic Deep Water and, 360–61, 362–63
 - thermodynamic control of, 227
- Density temperature, defined, 215
- Diabatic Acceleration and REscaling (DARE), 314, 316–17, 324–26
- Diabatic processes, 41, 60, 270
- Diurnal cycle biases, 307–8, 312–13
- Double ITCZ bias, 229, 244, 303–5
- Downdrafts, stratification and, 199
- Dynamical constraints, thermal stratification and, 49–53
- Dynamical time scale, baroclinic adjustment and, 27
- Eady growth-rate, 79
- Earth Radiation Budget Experiment (ERBE), 280, 308
- East Pacific Investigation of the Climate (EPIC), 226–27, 239
- Eddy diffusivity, structure of, 67
- Eddy lifecycle analysis, 37–40
- Eddy momentum fluxes
- forcing, dissipation and, 40–42
 - Hadley circulation and, 255
 - inviscid life cycles and, 37–40
 - thermal stratification and, 62–65
 - tropospheric dynamics and, 17
 - two-layer QG model and, 4
 - upper troposphere and, 17
- Eddy-mediated responses
- abrupt climate change and, 355–56
 - circulation constraint in upper atmosphere and, 257–61
 - dynamical mechanisms of, 125–27
 - low latitude-extratropical interactions and, 104–11, 137–39
 - mean flow state and, 22–23
 - structural circulation changes and, 127–33
 - theory of, 111–19
 - tropical forcing of annular modes and, 134–37
 - tropical warming and, 119–25
- Effective static stability, 12, 276, 285–87
- Ekman damping, 61, 85, 86–87, 93
- El Niño-Southern Oscillation (ENSO)
- abrupt climate change and, 353–55

- biases in, 302–3, 306
- changes following, 105, 106
- climate change and, 342, 353–55
- equatorial warming and, 106–8
- mechanisms for warming and, 290
- modeling of, 219–20, 270–72
- precipitation anomalies and, 110
- radiative cooling and, 292
- Southern Annular Mode (SAM) and, 134–37
- storm track dynamics and, 88
- wave dynamics and, 287, 289
- Eliassen-Palm flux, 81, 96, 115, 138
- Emission temperature, tropopause height and, 73–74
- Energy fluxes, FHZ idealized moist GCM and, 15–16
- Enthalpy flux, 188, 198
- Entropy flux, 10–11, 65–69
- Eocene, abrupt climate change and, 332
- Equatorial forcing, Rossby waves and, 104
- Equatorial superrotation, 128–33, 138–39
- Equivalent potential temperature, 231
- Evaporation fallacy, 153
- Feedbacks
 - cloud radiative, 285–87, 317–18
 - cloud-resolving models (CRMs) and, 317–24
 - eddy, 125–127
 - ice albedo, 147, 150–51
 - lapse-rate, 321
 - moisture-convection, 206
 - surface flux mechanisms and, 293
 - tropical perturbations and, 198–99
 - water vapor and, 52, 143–44
 - WISHE and, 204–5, 207, 214
- Ferrel cell, 61, 125
- Forcings
 - abrupt climate change and, 353
 - of annular modes, 134–37
 - baroclinic adjustment and, 27
 - cloud radiative, 285–87
 - eddy-mediated responses and, 40–42, 111
 - of equatorial waveguides, 204
 - planetary boundary layer (PBL) and, 244–45
 - potential vorticity gradients and, 42
 - radiative-convective equilibrium and, 189
 - storm track dynamics and, 98–101
- Free tropospheric humidity (FTH), 152–54
- General circulation models (GCMs). *See also* Atmospheric general circulation models (AGCMs); Coupled ocean-atmosphere general circulation models (CGCMs)
 - abrupt climate change and, 357–58
 - annular modes and, 134–36
 - biases in, 222, 312
 - eddies and, 23
 - ENSO and, 270–71
 - moisture convergence and, 222
 - orbital changes and, 332
 - relative humidity and, 143–44, 149–50, 177–79
 - storm track dynamics and, 91–92
 - temperature gradients and, 22
 - THC-driving theory and, 344–46
 - tropical warming and, 132
 - tropical-extratropical teleconnections and, 110, 123–24
 - two-layer QG dynamics and, 3
 - ventilation mechanism and, 283
- Geostrophic mass flux, 59–60, 61, 62–65
- Gill model, 202, 223–27
- Global warming. *See also* Abrupt climate change
 - AGCM response to, 318
 - changes in storm tracks and, 80
 - equatorial superrotation and, 138–39
 - midlatitude eddy fluxes and, 12
 - poleward displacement of surface westerlies and, 19
 - QTCM and, 279–80
 - relative humidity and, 143, 174–80
 - Southern Annular Mode (SAM) and, 136–37
 - tropical precipitation changes and, 272, 293–95
 - uncertainty in cloud feedback and, 317–24
 - water vapor and, 146
- GMS (gross moist stability) multiplier effect, 290, 291, 292

- Greenhouse gases, 146–47, 150–51
- Greenland, 333–35, 340
- GRIP, 334
- Gross moist stability. *See also* GMS (gross moist stability) multiplier effect
- fluctuations in, 56–58
 - intertropical convergence zones (ITCZs) and, 278, 296
 - overview of, 276–78
 - rich-get-richer mechanism and, 294
- Group propagation dynamics, storm tracks and, 82–84
- Gulf Stream, THC-driving theory and, 343–44
- Hadley cells
- abrupt climate change and, 355
 - ageostrophic mass flux and, 61
 - equatorial superrotation and, 131
 - extratropical temperature changes and, 124–25
 - jets and, 132–33
 - lack of symmetry in, 110
 - monsoon circulations and, 252
 - redistribution of heat by, 111
 - storm tracks, extratropical jet and, 41
 - temperature and, 122
 - tropical warming and, 125
 - zonal asymmetry and, 255
- Heat fluxes
- abrupt climate change and, 350–51, 361–62
 - Gill model and, 223
 - Hadley cells and, 111
 - potential vorticity and, 112–13
 - storm track dynamics and, 95–96
 - surface winds and, 225
 - WISHE and, 204–5, 207, 214
 - zonal-mean circulation anomalies and, 108
- Heinrich events, 365
- Held-Hou theory of Hadley circulation, 252–53
- Hoskins-Rodwell effect, 263, 282, 283
- Humidity, 206. *See also* Relative humidity
- Hurricanes, 204, 212–13, 230. *See also*
- Cyclones
- Hysteresis, 100, 130
- Ice albedo feedback, 147, 150–51
- Ice cores, 333–35, 340–41
- Ice microphysics, 310
- Ice sheets, 331, 332, 352–53
- Icelandic Low, 351, 353
- Idealized global climate models
- dry, 19, 27–28, 69–71
 - moist, 14–16
 - relative humidity and, 143–44
 - simulations using, 318–24
 - thermal stratification and, 22, 69–71
- Interactive Rodwell-Hoskins (IRH) mechanism, 282, 283
- Interior atmosphere, mean mass fluxes and, 60–61
- Intermediate models, abrupt climate change and, 348
- Intertropical convergence zone (ITCZ)
- abrupt climate change and, 337, 356, 357–58
 - double ITCZ bias and, 229, 244, 303–5
 - factors controlling, 220
 - gross moist stability and, 278, 296
 - moist static energy and, 279
 - precipitation and, 228–29
 - sea surface temperatures and, 240–43
 - surface winds and, 226–27
 - THC-driving theory and, 345
 - Younger Dryas and, 365
- Intransitive systems, 335, 363–64
- Inverse energy cascade, 6–7, 23
- Isentropic coordinates, 58
- Isentropic slope, 26, 29, 58–59. *See also* Static stability
- Jets
- abrupt climate change and, 355–60
 - eddy forcing and, 23
 - Hadley circulation and, 132–33
 - lower tropospheric eddies and, 261–64
 - meridional shift of, 108
 - momentum flux, convergence and, 39
 - tropical-extratropical teleconnections and, 127–33
- Kapingamarangi, 192
- Kelvinoid solution, 287–89, 292–93, 306

- La Niña, abrupt climate change and, 354
- Land convective zones, 280
- Land-ocean contrast, 280–84, 286–87
- Lapse-rate feedback, 321
- Last Glacial Maximum, 332, 338, 340, 347
- Latent heating, 12, 14, 16, 276
- Laurentide ice sheet, 352–53, 359–60
- Levy flights, 174
- Life-cycle studies, 22, 37–40, 133
- Lindzen-Nigam model, 224–28, 245–46
- Local modes, 5, 91–92
- Longwave cloud forcing, 308

- Macroturbulence, 1, 67
- Madden-Julian Oscillation (MJO), 186, 205, 212, 306–7, 315
- Markov processes, 174
- Mass fluxes, balance condition on, 59–65
- Matsuno model, 202, 223–27
- Maxwell's relations, 196
- Mean field theories, 89
- Mean meridional circulation (MMC), 38, 124, 137
- Mediation, convective quasi-equilibrium, 290, 291
- Meridional mass fluxes, 60, 61
- Methane records, 333
- Midwinter minimum in storm track activity, 80
- Miles-Howard condition, 28
- Mixing
 - drying, transport and, 158–63
 - interior vs. boundary, 33–37
 - thermal stratification and, 67
 - trajectory approach and, 154–55, 157–58
 - transport, drying and, 158–63
- Mixing length theory, 22–23, 35
- Mixing slope, 11
- Moist adiabat, defined, 192
- Moist adiabatic lapse rate, 53–54, 189, 191, 195–97, 199–200
- Moist available potential energy, 12, 13–14
- Moist convection. *See also* Global warming; Monsoons
 - baroclinic adjustment and, 27–28
 - challenges in modeling of, 206, 302–3
 - damping of, 203
 - precipitation anomalies and, 270–73, 279–80, 285, 289–93
 - static stability of midlatitudes and, 16
 - thermal stratification and, 49, 55–58
 - Tropics and, 52–53
- Moist criticality, 192
- Moist entropy, 230–31
- Moist static energy budget
 - land convective zones and, 280
 - land-sea contrast and, 280–81
 - large-scale advection and, 198
 - overview of, 273–79
 - precipitation and, 231–38, 245–46, 247
 - QTCM and, 279–80
 - surface flux mechanisms and, 293
 - as tracer, 312
 - ventilation mechanism and, 282
- Moist wave dynamics, 287–89, 291–92
- Moisture convergence, 206, 221, 222, 227, 276
- Moisture-convection feedback, 206
- Momentum fluxes
 - baroclinic adjustment and, 38
 - convergence and, 117, 229
 - entropy budget and, 10–11
 - equatorial superrotation and, 129
 - forcing and, 40–42
 - Hadley circulation and, 252, 255
 - jets and, 39
 - Kelvinoid solution and, 288
 - life-cycle studies and, 37–40, 133
 - limitation of surface winds and, 220
 - Lindzen-Nigam model and, 225
 - PBL control and, 228–29
 - precipitation and, 227–28
 - radiative-convective equilibrium and, 189
 - storm track dynamics and, 96–97
 - temperature and, 41, 62–65, 108
 - transient eddy heat fluxes and, 108
 - two-layer QG model and, 4
 - upper troposphere and, 17
 - vertical redistribution of, 38
 - vertical shear and, 39
 - zonal-mean circulation anomalies and, 108
- Monsoons
 - abrupt climate change and, 338, 345, 346
 - circulation constraint in upper atmosphere and, 253–56, 257–61

- dynamical constraints on, 252–53, 264–65
 - lower tropospheric eddies and, 261–64
 - nonlocal coupling of with deserts, 333
 - overview of, 268–70
 - setting of poleward boundaries for, 281–84
 - sustained divergent circulations and, 256–57
- Montgomery streamfunction/potential, 59, 255–56
- Multiplier effect, 290, 291, 293
- Multiscale modeling, 314–16
- Newtonian relaxation, 69, 93–94, 98
- Nigam-Lindzen model, 224–28, 245–46
- Nino 3.4 SST Index, 107, 135
- Non-locality problem, baroclinic adjustment and, 25
- Normal modes, 90–93
- North Atlantic Deep Water, 360–61, 362–63
- North Atlantic Ocean
- abrupt climate change and, 340–41, 349–50
 - Greenland sea surface temperatures and, 335
 - impact of shift to zonal circulation in winter and, 351–52
 - THC-driving theory and, 343–44, 345–46, 347
 - winter shift to zonal circulation and, 351–52
- Northern Annular Mode (NAM), 135–36, 342, 353
- Northern hemisphere, abrupt climate change and, 332
- Oceanic storm tracks, inviscid life cycle
- calculations and, 40
- Oceans. *See also* Deep ocean circulation; *Specific oceans*
- abrupt climate change and, 361
 - convective quasi-equilibrium and, 280–81, 284–85
 - coupling to, 206–7
 - radiative damping over, 293
 - tropical circulations and, 214
- Orbital changes, 331, 332, 354
- Outgoing longwave radiation (OLR)
- baroclinic adjustment and, 25
 - elevation and, 152
 - factors determining, 147–51
 - Madden-Julian Oscillation (MJO) bias and, 307
 - upper-level potential vorticity and, 258–59
 - water vapor and, 146–47
- Oxygen isotope analysis, 333–35, 338–39
- Pacific Ocean, THC-driving theory and, 345
- Parallel shear flow instability, 28
- Phase speed, storm structure and, 82
- Planetary boundary layer (PBL)
- East Pacific Investigation of the Climate (EPIC) studies and, 239
 - ENSO biases and, 306
 - mechanisms for destabilization of, 244–45
 - precipitation and, 227–29
 - surface winds and, 224–25
- Polar amplification, 147
- Polar front jet (PFJ), abrupt climate change and, 355–56
- Polar ice cores, 333–35, 340–41
- Potential vorticity
- baroclinic eddies and, 111–19
 - critical shear and, 29
 - divergent tropical flow and, 255–56
 - equatorial superrotation and, 130
 - forcing and, 42
 - mixing of interior, 34–37
 - quasigeostrophic conservation of, 112
 - static stability and, 33–34
 - storm track dynamics and, 86–87, 93–94
 - tropospheric dynamics and, 17
 - two-layer model and, 31–33
 - zonal asymmetry and, 253
- Prandtl problem, 188–89
- Precipitation
- cloud radiative feedbacks and, 285–87
 - diurnal cycle biases and, 307–8, 312–13
 - El Niño and, 110
 - at given sea surface temperatures, 219–20, 244–47
 - Lindzen-Nigam model and, 225
 - Madden-Julian Oscillation (MJO) bias and, 306–7
 - mechanisms for anomalies in with global warming, 293–95
 - moist convection and, 268
 - moist static energy and, 272–73, 284

- moist teleconnection and, 290
- monsoons and, 252, 268–70, 281–84
- PBL momentum control of, 228–29
- radiative-convective equilibrium and, 188–89
- theories for, 220–23, 227–28, 238–44
- thermodynamic control of, 230–38
- Probability density functions (PDF), 156–57, 164–66, 174–78
- Pseudo-adiabatic processes, 215
- Pseudomomentum, 96–97
- Quasi-equilibrium, 231, 289, 291. *See also*
 - Convective quasi-equilibrium
- Quasi-equilibrium tropical circulation model (QTCM)
 - defined, 220
 - ENSO and, 271–72
 - examples of application of, 210–11
 - formulation of hypothesis of, 190–91
 - overview of, 279–80
 - schematic representation of, 272
 - surface winds and, 223
 - theoretical and empirical bases for, 192–95
 - ventilation mechanism and, 283
- Radiation budget
 - equilibrium in, 187–90, 207–10
 - static stability and, 9–10, 25, 49–53
 - tropospheric humidity and, 152–53
 - water vapor and, 146, 147–51
- Radiative constraints, 25, 49–53
- Radiative equilibrium, 3, 52
- Radiative-convective equilibrium
 - baroclinic adjustment and, 27
 - departures from, 235
 - effect of departures from, 203
 - examples of closure and, 210–11
 - feedback of air motion on temperature and, 198–99
 - finite-amplitude perturbations and, 207–10
 - fixed sea surface temperature and, 202–3
 - humidity fluctuations and, 206
 - moist-adiabatic lapse rate, tropical disturbances and, 195–97
 - oceans and, 206–7
 - overview of, 50, 187–90
 - precipitation, local surface evaporation and, 220–21
 - quasi-linear equatorial system for first baroclinic mode and, 199–201
 - sea surface temperature anomalies and, 201–2
 - WISHE and, 204–5
- Random walk model, 169–70
- Reflection principle, 164
- Relative humidity
 - advection-condensation model and, 154
 - atmospheric saturation and, 151–58
 - climate change and, 174–79
 - diffusion-condensation model and, 159–63
 - fluctuations in, 206
 - forced equilibria and, 169–74
 - overview of, 143–45, 179–83
 - radiation budget and, 147–51
 - stochastic drying and, 163–69
 - thermal stratification and, 50
 - water vapor properties and, 145–47
- Relaxed equilibrium, defined, 191
- Rhines scale, 14, 15, 18
- Rich-get-richer mechanism, 294, 295
- Rodwell-Hoskins effect, 263, 282, 283
- Rossby radius, 23
- Rossby waves
 - baroclinic eddies as linear, 126–27
 - ENSO and, 136, 137, 306
 - Equatorial forcing and, 104
 - equatorial superrotation and, 129
 - interactive Rodwell-Hoskins (IRH) mechanism and, 282
 - potential vorticity gradients and, 17
 - storm track dynamics and, 81, 95
- Sahara, greening of, 332
- Sajama, 338
- Salinity, 340, 357
- Saturation deficit, moist eddies and, 13
- Saturation fallacy, 153
- Saturation moist entropy, 54, 195
- Saturation specific humidity, 145, 158, 180
- Saturation vapor pressure, 145
- Sea ice, abrupt climate change and, 349–50
- Sea surface temperatures

- abrupt climate change and, 335–36, 339, 352
- anomalies in, equilibrium and, 201–2
- El Niño and, 105, 106, 107
- fixed, equilibrium and, 202–3
- idealized Walker circulation CRM simulations and, 320–24
- moist static energy budget and, 284–85
- precipitation and surface wind modeling and, 219–20, 244–47
- Southern Annular Mode (SAM) and, 134
- surface flux mechanisms and, 293
- teleconnection and, 291, 293
- tropical circulations and, 210, 214
- tropical warming and, 119–25
- warm eastern ocean/double ITCZ bias and, 304–5
- Shear, 28–33, 189, 190
- Shear flow instability, 28
- Shortwave cloud forcing, 308
- Shortwave cutoff, 40
- Slantwise convection, 53–55, 71, 74
- Snowball Earth, 149, 150
- Source of wave activity, 96–97
- Southern Annular Mode (SAM), 110, 134–37
- Southern Hemisphere, abrupt climate change and, 332, 338–39
- Specific humidity, moist static energy and, 272–73
- Speleothems, 337, 338
- Stability, 230–31. *See also* Gross moist stability; Static stability
- Stalactites and stalagmites, 337, 338
- Static energy. *See* Moist static energy budget
- Static stability
 - baroclinic adjustment and, 33–34, 39
 - effective, 12, 276, 285–87
 - isentropic slope and, 11
 - of midlatitudes, latent heating and, 16
 - moist convection and, 56
 - thermal stratification and, 68
 - two-layer QG model and, 4, 9–10
- Stationary waves, 85, 136
- Steering level, potential vorticity gradients and, 37
- Stochastic forcing, 23, 163–69, 169–74
- Stochastic models, storm track dynamics and, 93–95
- Storm tracks
 - abrupt climate change and, 355–60
 - heuristic models for, 95–98
 - linear theories for, 89–90
 - nonlinear behavior of, 98–101
 - normal modes and, 90–93
 - overview of, 78–84, 101–2
 - perturbations in, 88–89
 - stochastic models for, 93–95
 - tropical-extratropical teleconnections and, 127–33
 - variability example for, 84–88
- Stratosphere, 52, 137
- Strict equilibrium, 191, 203
- Subtropical jet (STJ), 355–56
- Supercooling, 192
- Supercriticality
 - insensitivity of to changes in forcing, 31–32
 - overview of, 28–29
 - storm track dynamics and, 98–100
 - thermal stratification and, 65–70, 72–73
 - two-layer QG model and, 3, 42
- Superparameterization, 314–16
- Superrotation, 128–33, 138–39
- Surface processes, baroclinic adjustment and, 40
- Surface temperature, tropopause height and, 50–53
- Surface winds
 - ENSO biases and, 306
 - Gill model for, 223–24, 225–26
 - at given sea surface temperatures, 219–20, 244–47
 - Lindzen-Nigam model and, 224–26
 - moist static energy and, 234
 - precipitation and, 220
 - theories for, 220–23
 - warm eastern ocean/double ITCZ bias and, 304–5
- Synoptic development, 26–27
- Synoptic eddy life cycles, 81
- Teleconnections, 270–73, 279–80, 285, 289–93

- Temperature
- convective quasi-equilibrium constraint and, 278–79
 - entropy budget and, 10–11
 - evaporation and, 153
 - feedback of air motion, equilibrium and, 198–99
 - of free troposphere, 201
 - gross moist stability and, 276
 - moist convection and, 268
 - moist static energy and, 272–73
 - oxygen isotopes as proxy for, 333–35
 - relative humidity and, 149
 - saturation vapor pressure and, 145
 - transient eddy heat and momentum fluxes and, 108
 - tropical soundings of, 192–93
 - water vapor, climate change and, 147
- Thermal stratification
- baroclinic eddies and, 58–65
 - baroclinic entropy flux, supercriticality and, 65–69
 - eddy scale reduction and, 34
 - factors determining, 22–24, 49–73
 - moist convection, baroclinic eddies and, 55–58
 - radiative and dynamical constraints on, 49–53
 - simulations with idealized GCM and, 69–71
 - slantwise convection and, 53–55
 - two-layer QG model and, 5
- Thermocline depth, 360
- Thermodynamic control, 230–38, 244
- Thermodynamic disequilibrium, 204
- Thermohaline circulation (THC)
- abrupt climate change and, 332, 353, 354, 357–58
 - deep water formation and, 339–40
 - impact of shift to zonal circulation in winter and, 352
 - overview of, 343–44
 - sea ice and, 349–50
 - spatial pattern of, 344–47
 - temporal behavior of, 347–48
- Thermostat theory, 26
- Tibetan anticyclone, 253, 255–56, 258–60
- Time of last saturation model, 154
- Topography, storm track dynamics and, 98
- Trajectory approach, 154–58, 174–77, 182
- Transformed Eulerian mean (TEM)
- circulation, 115, 117–19, 124, 138
- Transient eddies
- abrupt climate change and, 350–51, 355–56
 - mean meridional circulation (MMC) and, 124
 - storm track dynamics and, 81–84, 86–87, 92, 95–96
 - thermal stratification and, 55–69
 - zonal-mean circulation anomalies and, 108
- Transport, mixing, drying and, 158–63
- Tropical-extratropical teleconnections
- dynamical mechanisms of, 125–27
 - eddy-mediated, 104–11, 137–39
 - structural circulation changes and, 127–33
 - theory of eddy-mediated, 111–19
 - tropical forcing of annular modes and, 134–37
 - tropical warming and, 119–25
- Tropics. *See also* Radiative-convective equilibrium
- abrupt climate change and, 332, 336–37, 338–39, 353, 355–60
 - cyclones of, 210, 211–13
 - dry air and, 151
 - greenhouse effect and, 148–49
 - Hadley cell responses in, 111, 122
 - limitations on data collection in, 186
 - moist convection and, 52–53
 - moist teleconnection mechanisms in, 289–93
 - moist-adiabatic lapse rate, disturbances and, 195–97
 - overview of quasi-equilibrium dynamics of, 186–87, 213–15
 - red spectrum of, 203, 204
 - responses of idealized models to warming in, 119–25
 - Rossby waves and, 104
 - tropopause height and, 74
- Tropopause
- boundary layer theories and, 48
 - moist adiabatic lapse rate and, 200
 - as rigid lid, 199, 204, 212

- static stability and, 10
- surface temperature, tropospheric lapse rate and, 50–53
- Troposphere/SST disequilibrium mechanisms, 291, 293
- Turbulence, baroclinic forcing and, 98
- Two-box model, 207–10
- Two-layer QG model
 - critical shear of, 28–33
 - eddy closure in, 4–5
 - entropy budget and, 10–11
 - homogeneous limit and, 5–9
 - overview of, 2–4
 - static stability and, 9–10
 - storm tracks and, 84–93
- Upped-ante mechanism, 290–91, 292, 294, 295
- Upper tropospheric humidity, 152–54
- Variability, storm tracks and, 79–80
- Venezuela, 336–37, 339, 345
- Ventilation mechanism, 282–84, 295
- Vertical shear, 25–26, 39, 41, 79
- Walker circulation model, 207–10, 319–22
- Water vapor. *See also* Relative humidity
 - basic properties of, 145–47
 - cloud-radiation interactions and, 205–6
 - feedback modeling and, 143–44
 - radiation budget and, 147–51
 - tropopause height and, 52
 - two-layer QG model and, 12
- Wave dynamics, moist teleconnection and, 289, 291
- Waveguides, 89, 95–97, 127, 204, 211
- Weak temperature gradient (WTG) approximation, 230
- Webster model, 202, 223–27
- Wind-evaporation feedback, 204–5, 207, 214
- Wind-induced surface heat exchange (WISHE), 204–5, 207, 214
- Winter, storm tracks and, 80, 85
- Younger Dryas. *See* Abrupt climate change
- Zonal asymmetry
 - Hadley circulation and, 252–53, 255
 - Lindzen-Nigam model and, 224
 - Southern Annular Mode (SAM) and, 136–37
 - storm track dynamics and, 85–86, 90–93, 97–98